Comparative study of macroscopic traffic flow models at road junctions

Paola Goatin, Elena Rossi

▶ **To cite this version:**

Paola Goatin, Elena Rossi. Comparative study of macroscopic traffic flow models at road junctions. Networks and Heterogeneous Media, 2020, 15 (2), pp.261-279. hal-02474650

HAL Id: hal-02474650
https://hal.science/hal-02474650

Submitted on 11 Feb 2020

HAL is a multi-disciplinary open access archive for the deposit and dissemination of scientific research documents, whether they are published or not. The documents may come from teaching and research institutions in France or abroad, or from public or private research centers.

L'archive ouverte pluridisciplinaire **HAL**, est destinée au dépôt et à la diffusion de documents scientifiques de niveau recherche, publiés ou non, émanant des établissements d'enseignement et de recherche français ou étrangers, des laboratoires publics ou privés.

Comparative study of macroscopic traffic flow models at road junctions

Paola Goatin[1] Elena Rossi[2]

February 11, 2020

Abstract

We qualitatively compare the solutions of a multilane model with those produced by the classical Lighthill-Whitham-Richards equation with suitable coupling conditions at simple road junctions. The numerical simulations are based on the Godunov and upwind schemes. Several tests illustrate the models' behaviour in different realistic situations.

2010 Mathematics Subject Classification: 35L65, 90B20, 82B21.

Keywords: macroscopic traffic flow models on networks; multilane models; multi-population models; finite volume schemes.

1 Introduction

Starting form the well-known Lighthill-Whitham-Richards (LWR) model [17, 18], a variety of macroscopic traffic flow models based on hyperbolic balance laws have been proposed to capture traffic behaviour in different situations. In this paper, we focus on the description of traffic dynamics on road networks. More precisely, we investigate the role of coupling conditions at road junctions. To this aim, we compare the behaviour of the multilane junction model introduced in [13], and the classical LWR model at junctions [10, Chapter 5].

The multilane junction model [13] allows to handle in detail various realistic cases of road junctions, with the major exception of the diverging ones, which requires some additional information on drivers' routing preferences upstream. To avoid cumbersome notation, we recap here the main features of the multilane model in the case of a junction consisting of 2 incoming roads and 1 outgoing road, the number of lanes in each road to be specified later. Let $M_\ell = M_{\ell_1} + M_{\ell_2}$ be the number of lanes on the half line $x < 0$, M_{ℓ_j} being the number of lanes on the j-th incoming road, $j = 1, 2$. Similarly, let M_r be the number of lanes on $x > 0$, corresponding to the outgoing road. Each lane has maximal possible density normalized to 1, but each road may have different maximal speed. The detailed model is described in Section 3 below. Clearly, the case of a 1-to-1 junction is included, but not the 1-to-2 junction. This specific situation will be addressed separately in Section 5.

[1]Inria Sophia Antipolis - Méditerranée, Université Côte d'Azur, Inria, CNRS, LJAD, 2004 route des Lucioles - BP 93, 06902 Sophia Antipolis Cedex, France. E-mail: paola.goatin@inria.fr

[2]Università degli Studi di Milano-Bicocca, Dipartimento di Matematica e Applicazioni, via R. Cozzi 55, 20126 Milano, Italy. E-mail: elena.rossi@unimib.it The author is a member of INdAM-GNAMPA (Gruppo Nazionale per l'Analisi Matematica, la Probabilità e le loro Applicazioni).

In order to draw a comparison with the LWR model on networks, we *sum* the vehicle densities on the various lanes, and we compare the total density profile with the solution given by the LWR model with corresponding maximal density. Notice that, in this way, we are led to consider the LWR model at a 2-to-1 junction with maximal density M_{ℓ_j} on the j-th incoming road and M_r on the outgoing road. This choice is driven by the fundamental principle of conservation of the number of vehicles across the junction. The same approach is used on diverging junctions.

The numerical tests described in Sections 4 and 5 point out similarities and differences between the multilane model and its LWR counterpart. Interestingly, in the case of a 1-to-1 junction, the multilane description captures a different behaviour than those commonly described by the classical LWR approach. Merging junctions display pretty the same dynamics with both approaches, while diverging junctions show a more complex behaviour, acting as FIFO (first-in-first-out) when one outgoing road is fully congested, and as non-FIFO otherwise. Further assessment on the validity of the models necessitate the comparison with suitable real data.

2 LWR on n-to-m junctions

We recall the LWR model on n to m junctions, that is on junctions with n incoming roads and m outgoing roads. More details can be found in [8, 10].

A road network is modelled by a finite collection of edges and vertices, representing respectively unidirectional roads and junctions. On each edge I, and thus on each road, traffic flow is described through the Lighthill-Whitham-Richards (LWR) model: the density of vehicles $\rho(t,x)$ satisfies

$$\begin{cases} \partial_t \rho + \partial_x f_I(\rho) = 0, \\ \rho(0,x) = \rho_o(x), \end{cases} \tag{2.1}$$

where f_I is assumed to be strictly concave and of class $\mathbf{C^2}$, such that $f(0) = f(R_I) = 0$, R_I being the maximal possible density on road I. In particular, we may choose

$$f_I(u) = V_I\, u \left(1 - \frac{u}{R_I}\right), \tag{2.2}$$

where V_I is the maximal speed on road I. Note that, with this particular choice of flux, f_I attains its unique maximum at $\vartheta_I = R_I/2$. At network junctions, the conservation of the number of vehicles has to be ensured and, moreover, the usual choice is to maximise the flux through the junction. We introduce therefore the demand and supply functions (see for instance [12]) and express the flux at the junction through an *ad hoc* minimisation between the two:

$$D_I(u) = \begin{cases} f_I(u) & \text{if } u \le \vartheta_I, \\ f_I(\vartheta_I) & \text{if } u \ge \vartheta_I, \end{cases} \quad \text{and} \quad S_I(u) = \begin{cases} f_I(\vartheta_I) & \text{if } u \le \vartheta_I, \\ f_I(u) & \text{if } u \ge \vartheta_I. \end{cases} \tag{2.3}$$

The demand and supply functions introduced above are displayed in Figure 1.
Notice that, as in [12], the flux function f_I, as well as the corresponding demand and supply functions, may depend also on time, if traffic regulations are applied.

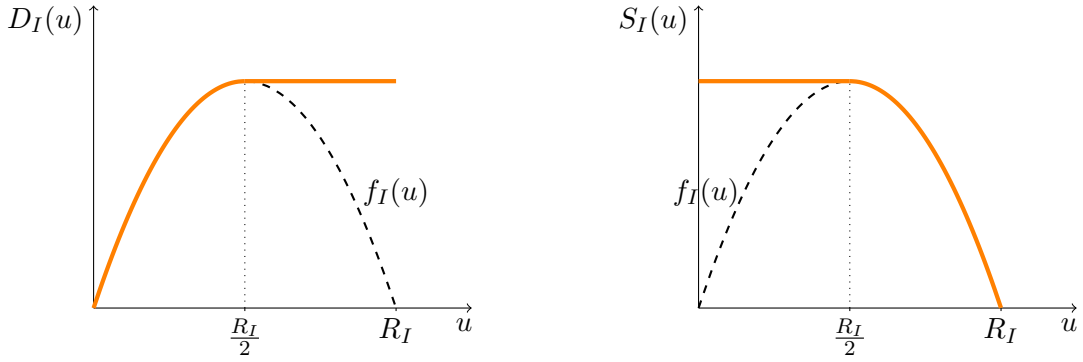

Figure 1: The demand (left) and supply (right) function for f_I as in (2.2). In both pictures, the dashed line represents $f_I(u)$.

At each junction, the model includes also of the preferences of the drivers, which are prescribed and known *a priori*. These preferences describe the distribution of traffic from incoming to outgoing roads and are expressed as elements of a matrix A, called *traffic distribution matrix*: for a vertex J with n incoming edges $I_1, \dots, I_n$ and m outgoing edges $I_{n+1}, \dots, I_{n+m}$, the matrix A is given as follows

$$A = (a_{j,i}) \in \mathbb{R}^{m\times n} \quad \text{with } 0 \le a_{j,i} \le 1 \text{ for every } i \in \{1,\dots,n\} \text{ and } j \in \{n+1,\dots,n+m\}$$
$$\text{and} \sum_{j=n+1}^{n+m} a_{j,i} = 1 \text{ for every } i \in \{1,\dots,n\}\,.$$

In other words, each element $a_{j,i}$ of the matrix A gives the percentage of traffic from road I_i going into road I_j at the junction.

In view of the examples considered in this paper, we focus on the cases of one-to-one junctions (modeling speed limit or lane number changes), two-to-one (merging) junctions and one-to-two (diverging) junctions, see Figure 2. In the case of merging junctions, where the

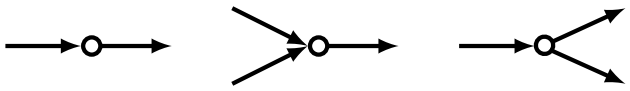

One-to-one Two-to-one One-to-two

Figure 2: The types of junction considered in this work for the LWR model.

number of incoming roads is greater than the number of outgoing roads, it is necessary to introduce a priority parameter for each incoming road to single out a unique solution. In particular, for two-to-one junctions, the two incoming roads are characterised by the priority parameters P and $(1-P)$, with $P \in]0,1[$.

2.1 1-to-1 junction

Consider a one-to-one junction and call I_1, I_2 respectively the incoming and outgoing road. Denote by ρ_i the density of vehicles in road I_i, $i = 1, 2$. Observe that the LWR model (2.1)

on this particular junction is equivalent to a Cauchy problem for a conservation law with discontinuous flux (see, for instance, [14, Chapter 8] for a brief introduction to the topic):

$$\begin{cases} \partial_t \rho + \partial_x f(x,\rho) = 0, \\ \rho(0,x) = \rho_o(x), \end{cases} \tag{2.4}$$

with

$$v(x,u) = H(x)\, v_r(u) + (1 - H(x))\, v_\ell(u), \tag{2.5}$$

$$f_\ell(u) = u\, v_\ell(u) \qquad f_r(u) = u\, v_r(u), \tag{2.6}$$

$$f(x,u) = u\, v(x,u) = H(x)\, f_r(u) + (1 - H(x))\, f_\ell(u), \tag{2.7}$$

H being the Heaviside function. The functions v_ℓ and v_r are strictly decreasing, positive and such that $v_d(R_d) = 0$ for $d = \ell, r$. One admissible choice is

$$v_d(u) = V_d \left(1 - \frac{u}{R_d}\right), \tag{2.8}$$

for a suitable positive constant V_d, leading to the flux function (2.2).

Concerning the initial datum ρ_o, it satisfies the following constraints:

$$\rho_o(x) \in [0, R_\ell] \text{ for } x \in]-\infty, 0[, \qquad \rho_o(x) \in [0, R_r] \text{ for } x \in]0, +\infty[.$$

Hyperbolic conservation laws with discontinuous flux such as (2.4) arise in the modelling of several phenomena, such as, for instance, two phase flow in heterogeneous media and traffic flow with rough road conditions. Among the rich literature on the subject, we refer the interested reader to [2, 3, 6, 16, 21] and the references therein.
The main issue when dealing with conservation laws with discontinuous flux function is the lack of a unique solution, since the classical theory by Kružkov does not apply. Clearly, Kružkov entropy conditions are valid away from the point(s) of discontinuity of the flux, but they are not enough to provide the uniqueness of solution. With the aim of proving the well-posedness of the problem, various notions of solutions have been introduced in the literature, based of different admissibility conditions. We recall for example the *minimal variation* criterion introduced by Gimse and Risebro [11] and the Γ-*condition* described by Diehl [5]. We refer to [3] for a more complete overview.

In the present study, we will focus on the solutions given by the supply-demand flux maximizing criterion classically used in traffic flow modeling (satisfying the entropy criterion of [1]) and by the vanishing viscosity limit [6].

2.2 2-to-1 junction

In the case of merging junctions, a priority parameter has to be assigned to each incoming road, see [10, Section 5.2.2]. Therefore, in the specific situation of a two-to-one junction, the two incoming roads have priority P and $1 - P$ respectively, with $P \in]0, 1[$. The idea is that, in general, not all vehicles can pass at the junction: denoting by γ the amount of vehicles that can enter the outgoing road in the supply-limited case, $P\,\gamma$ vehicles comes from the first incoming road, and $(1 - P)\,\gamma$ cars from the second incoming road.

Clearly, since there is only one outgoing road, the traffic distribution matrix A reduces to the two-dimensional vector $(1, 1)$.

The initial datum satisfies the following constraints:

$$\begin{aligned} &\rho_{o,\ell_1}(x) \in [0, R_{\ell_1}] \text{ for } x \in]-\infty, 0[, \\ &\rho_{o,\ell_2}(x) \in [0, R_{\ell_2}] \text{ for } x \in]-\infty, 0[, \end{aligned} \qquad \rho_{o,r}(x) \in [0, R_r] \text{ for } x \in]0, +\infty[.$$

Following [12], denoting by ρ_{ℓ_i} and $\hat{\gamma}_{\ell_i}$ the density and the flux on the incoming roads ($i = 1, 2$) and by ρ_r, $\hat{\gamma}_r$ the density and the flux on the outgoing one, for $P \in]0, 1[$ the fluxes at the junctions are defined as

$$\begin{aligned} \hat{\gamma}_{\ell_1}(\rho_{\ell_1}, \rho_{\ell_2}, \rho_r) &:= \min\Big\{D_{\ell_1}(\rho_{\ell_1}), \max\big\{P\, S_r(\rho_r), S_r(\rho_r) - D_{\ell_2}(\rho_{\ell_2})\big\}\Big\}, \\ \hat{\gamma}_{\ell_2}(\rho_{\ell_1}, \rho_{\ell_2}, \rho_r) &:= \min\Big\{D_{\ell_2}(\rho_{\ell_2}), \max\big\{(1-P)\, S_r(\rho_r), S_r(\rho_r) - D_{\ell_1}(\rho_{\ell_1})\big\}\Big\}, \\ \hat{\gamma}_r(\rho_{\ell_1}, \rho_{\ell_2}, \rho_r) &:= \hat{\gamma}_{\ell_1}(\rho_{\ell_1}, \rho_{\ell_2}, \rho_r) + \hat{\gamma}_{\ell_2}(\rho_{\ell_1}, \rho_{\ell_2}, \rho_r). \end{aligned} \tag{2.9}$$

2.3 1-to-2 junction

The one-to-two junction is a particular diverging junction, see [10, Section 5.2.1] for more details. (Since there is only one incoming road, there is no need to prescribe a right of way.) In this case, the traffic distribution matrix A is given by:

$$A = \begin{bmatrix} \alpha \\ 1-\alpha \end{bmatrix}, \qquad \text{with } \alpha \in]0, 1[.$$

In [10] a FIFO (first-in-first-out) rule is applied at the junction. In terms of the demand and supply functions (2.3), the FIFO rule amounts to the following: denoting by ρ_ℓ the density on the incoming road, by ρ_{r_1} and ρ_{r_2} the densities on the outgoing roads, by γ_ℓ, γ_{r_1} and γ_{r_2} the fluxes on the incoming and outgoing roads respectively, we have

$$\begin{aligned} \gamma_\ell(\rho_\ell, \rho_{r_1}, \rho_{r_2}) &:= \min\left\{D_\ell(\rho_\ell),\ \frac{S_{r_1}(\rho_{r_1})}{\alpha},\ \frac{S_{r_2}(\rho_{r_2})}{1-\alpha}\right\}, \\ \gamma_{r_1}(\rho_\ell, \rho_{r_1}, \rho_{r_2}) &:= \alpha\, \gamma_\ell(\rho_\ell, \rho_{r_1}, \rho_{r_2}), \\ \gamma_{r_2}(\rho_\ell, \rho_{r_1}, \rho_{r_2}) &:= (1-\alpha)\, \gamma_\ell(\rho_\ell, \rho_{r_1}, \rho_{r_2}). \end{aligned} \tag{2.10}$$

As a consequence, if one of the outgoing roads is fully congested (i.e. $\min\{S_{r_1}(\rho_{r_1}), S_{r_2}(\rho_{r_2})\} = 0$), the vehicles are stuck at the junction ($\gamma_\ell = \gamma_{r_1} = \gamma_{r_2} = 0$), even if some of them could proceed in the other outgoing road. In order to overcome this problem, non-FIFO models have been developed, see for instance [12]. Non-FIFO model allows some flow through the junction even if one of the outgoing road is fully congested. Using the same notation as before, the non-FIFO rule reads as follows, in terms of the demand and supply functions (2.3):

$$\begin{aligned} \gamma_{r_1}(\rho_\ell, \rho_{r_1}, \rho_{r_2}) &:= \min\big\{\alpha\, D_\ell(\rho_\ell), S_{r_1}(\rho_{r_1})\big\}, \\ \gamma_{r_2}(\rho_\ell, \rho_{r_1}, \rho_{r_2}) &:= \min\big\{(1-\alpha)\, D_\ell(\rho_\ell), S_{r_2}(\rho_{r_2})\big\}, \\ \gamma_\ell(\rho_\ell, \rho_{r_1}, \rho_{r_2}) &:= \gamma_{r_1}(\rho_\ell, \rho_{r_1}, \rho_{r_2}) + \gamma_{r_2}(\rho_\ell, \rho_{r_1}, \rho_{r_2}). \end{aligned} \tag{2.11}$$

In the case of a diverging junction, the initial datum satisfies the following constraints:

$$\rho_{o,\ell}(x) \in [0, R_\ell] \text{ for } x \in]-\infty, 0[, \qquad \begin{array}{l} \rho_{o,r_1}(x) \in [0, R_{r_1}] \text{ for } x \in]0, +\infty[, \\ \rho_{o,r_2}(x) \in [0, R_{r_2}] \text{ for } x \in]0, +\infty[. \end{array}$$

3 A multilane model for n-to-1 junctions ($n = 1, 2$)

We recall the main features of the multilane junction model introduced in [13], based on the multilane traffic flow model proposed in [15]. The model provides a description of traffic on road networks with several lanes, allowing for lane changes and overtaking, as well as change in the speed laws and in the number of lanes along the road. In particular, $\mathcal{M}_\ell \subset \mathbb{N}^+$ represents the set of indexes of the *active* lanes on $]-\infty, 0[$, with cardinality $M_\ell = |\mathcal{M}_\ell| \geq 1$; on the other hand, $\mathcal{M}_r \subset \mathbb{N}^+$ is the set of indexes of the *active* lanes on $]0, +\infty[$, with cardinality $M_r = |\mathcal{M}_r| \geq 1$. We let $M \geq \max\{M_\ell, M_r\}$, its choice depending on the specific situation considered, and we assume, for technical needs, that there are $M - M_\ell$ and $M - M_r$ additional *phantom* lanes on $]-\infty, 0[$ and $]0, +\infty[$ respectively. We add moreover a condition (see (3.8) below), which prevents vehicles from passing from the active to the fictive lanes.

The model reads then as follows: for $x \in \mathbb{R}$ and $t > 0$, the vehicle density on lane j, $\rho_j = \rho_j(t, x)$, solves the Cauchy problem

$$\begin{cases} \partial_t \rho_j + \partial_x f_j(x, \rho_j) = G_{j-1}(x, \rho_{j-1}, \rho_j) - G_j(x, \rho_j, \rho_{j+1}), & j = \ldots, M, \\ \rho_j(0, x) = \rho_{o,j}(x), & j = \ldots, M, \end{cases} \tag{3.1}$$

with, for $j = 1, \ldots, M$,

$$v_j(x, u) = H(x)\, v_{r,j}(u) + (1 - H(x))\, v_{\ell,j}(u), \tag{3.2}$$

$$f_{\ell,j}(u) = u\, v_{\ell,j}(u), \qquad f_{r,j}(u) = u\, v_{r,j}(u), \tag{3.3}$$

$$f_j(x, u) = u\, v_j(x, u) = H(x)\, f_{r,j}(u) + (1 - H(x))\, f_{\ell,j}(u), \tag{3.4}$$

H being the Heaviside function. The velocities $v_{d,j}$, for $d = \ell, r$ and $j = 1, \ldots, M$, are strictly decreasing positive functions such that $v_{d,j}(1) = 0$. We assume that each map $f_{d,j}(u) = u\, v_{d,j}(u)$ admits a unique global maximum attained at $u = \vartheta_d^j$.

We set $\rho_{o,j} : \mathbb{R} \to [0, 1]$ for $j = 1, \ldots, M$ and

$$\rho_{o,j}(x) = 0 \quad \text{for } x \in]-\infty, 0[\text{ and } j \notin \mathcal{M}_\ell, \tag{3.5}$$

$$\rho_{o,j}(x) = 1 \quad \text{for } x \in]0, +\infty[\text{ and } j \notin \mathcal{M}_r. \tag{3.6}$$

The source terms, which account for the flow rates across lanes, are defined as in [15]:

$$\begin{aligned} G_{d,j}(\rho_j, \rho_{j+1}) &= K \left[\big(v_{d,j+1}(\rho_{j+1}) - v_{d,j}(\rho_j)\big)^+ \rho_j - \big(v_{d,j+1}(\rho_{j+1}) - v_{d,j}(\rho_j)\big)^- \rho_{j+1} \right] \\ &= K \left(v_{d,j+1}(\rho_{j+1}) - v_{d,j}(\rho_j)\right) \cdot \begin{cases} \rho_j & \text{if } v_{d,j+1}(\rho_{j+1}) \geq v_{d,j}(\rho_j), \\ \rho_{j+1} & \text{if } v_{d,j+1}(\rho_{j+1}) < v_{d,j}(\rho_j), \end{cases} \end{aligned} \tag{3.7}$$

for $d = \ell, r$ and $j = 1, \dots, M-1$, where $(a)^+ = \max\{a, 0\}$ and $a^- = -\min\{a, 0\}$ and K is a dimensional constant $(1/m)$, which can be assumed equal to 1 after rescaling space and time. To account for separate lanes, such as different roads or fictive lanes, we set

$$G_{d,j_d}(u, w) = 0 \qquad \text{for some } j_d \in \{1, \dots, M-1\}\,,\ d = \ell, r. \tag{3.8}$$

The functions appearing in the source term of (3.1) are then defined as follows

$$G_j(x, u, w) = H(x)\, G_{r,j}(u, w) + (1 - H(x))\, G_{\ell,j}(u, w) \qquad \text{for } j = 1, \dots, M-1, \tag{3.9}$$

$$G_0(x, u, w) = G_M(x, u, w) = 0. \tag{3.10}$$

For the sake of brevity, we introduce the notation $\boldsymbol{\rho} = (\rho_1, \dots, \rho_M)$, so that the initial data associated to problem (3.1)–(3.5)–(3.6) read $\boldsymbol{\rho}(0, x) = \boldsymbol{\rho}_o(x)$.

For simplicity, and with slight abuse of notation, we consider $\boldsymbol{\rho} = \boldsymbol{\rho}(t, x)$ for $t > 0$, $x \in \mathbb{R}$. However, as shown in [13], by (3.5), (3.6) and (3.8), there holds $\rho_j(t, x) = 0$ for all $t > 0$, $x \in]-\infty, 0[$ and $j \notin \mathcal{M}_\ell$, respectively $\rho_j(t, x) = 1$ for all $t > 0$, $x \in]0, +\infty[$ and $j \notin \mathcal{M}_r$.

In order to compare the multilane model to the LWR model at junctions, we make the following choices. In all the numerical experiments, for the multilane model we choose

$$v_{I,j}(u) = V_I\,(1 - u) \quad \text{for } j = 1, \dots, M,$$

with $V_I > 0$. Therefore, the maximal speed is the same for all lanes before, respectively after, $x = 0$. This corresponds to the following velocity for the LWR model:

$$v_I(u) = V_I\,\left(1 - \frac{u}{M_I}\right),$$

where M_I is the cardinality of the *active* lanes.

Through our numerical integrations, we show that the outcome may be different when not considering the number of lanes involved.

4 Comparison study

We compare now numerically the solution given by the multilane n-to-1 model with the corresponding LWR solutions. We first describe the numerical schemes used to compute approximate solutions of the considered models. Then we report on some numerical tests, which illustrates the behaviour of solutions in different cases.

4.1 Numerical schemes

We provide in this section the details on the numerical schemes used throughout the paper.

We introduce a uniform mesh in space, of width Δx, and a time step Δt, subject to a suitable CFL condition. For $k \in \mathbb{Z}$ set

$$x_k = \left(k + \frac{1}{2}\right)\Delta x, \qquad\qquad x_{k-1/2} = k\,\Delta x,$$

where x_k is the centre of the cell and $x_{k\pm1/2}$ its interfaces. Notice that nonnegative integers denote the cells on the positive part of the x-axis. Set $\lambda = \Delta t/\Delta x$. For the multilane model, we approximate the initial data as follows: for $j = 1, \dots, M$

$$\rho^0_{j,k} = \frac{1}{\Delta x} \int_{x_{k-1/2}}^{x_{k+1/2}} \rho_{o,j}(x)\,\mathrm{d}x\,, \tag{4.1}$$

recalling that (3.5) and (3.6) hold. The approximated initial data for the LWR model is given consequently as the sum of the initial data on various lanes, depending on the configuration under consideration:

- **1-to-1 junction (Section 4.2):** the initial data for the LWR model is merely given by the sum, thus

$$\rho^0_k = \sum_{j=1}^{M_\ell} \rho^0_{j,k} \quad \text{for } k \le -1; \qquad\qquad \rho^0_k = \sum_{j=1}^{M_r} \rho^0_{j,k} \quad \text{for } k \ge 0.$$

- **2-to-1 junction (Section 4.3):** for the merging junction, there are two incoming and one outgoing roads:

$$\begin{aligned} &\text{for } k \le -1: && \rho^0_{\ell_i,k} = \sum_{j=1}^{M_{\ell_i}} \rho^0_{j,k} \quad \text{for } i = 1, 2;\\ &\text{for } k \ge 0: && \rho^0_{r,k} = \sum_{j=1}^{M_r} \rho^0_{j,k}. \end{aligned}$$

- **1-to-2 junction (Section 5):** for the diverging junction, there are one incoming and two outgoing roads:

$$\begin{aligned} &\text{for } k \le -1: && \rho^0_{\ell,k} = \sum_{j=1}^{M_\ell} \rho^0_{j,k};\\ &\text{for } k \ge 0: && \rho^0_{r_i,k} = \sum_{j=1}^{M_{r_i}} \rho^0_{j,k} \quad \text{for } i = 1, 2. \end{aligned}$$

The solution to the multilane model (3.1)–(3.5)–(3.6)–(3.8) is obtained through a Godunov type scheme, with fractional step to take into account the source terms, see [13, Algorithm 2.1]:

$$\begin{aligned} \rho^{n+1/2}_{j,k} &= \rho^n_{j,k} - \lambda \left[F_j(x_{k+1/2}, \rho^n_{j,k}, \rho^n_{j,k+1}) - F_j(x_{k-1/2}, \rho^n_{j,k-1}, \rho^n_{j,k}) \right],\\ \rho^{n+1}_{j,k} &= \rho^{n+1/2}_{j,k} + \Delta t\, G_{j-1}(x_k, \rho^{n+1/2}_{j-1,k}, \rho^{n+1/2}_{j,k}) - \Delta t\, G_j(x_k, \rho^{n+1/2}_{j,k}, \rho^{n+1/2}_{j+1,k}), \end{aligned}$$

where

$$F_j(x,u,w) = \begin{cases} \min\left\{ D_j(x,u), S_j(x,w) \right\} & \text{if } x \neq 0,\\ \min\left\{ D_{\ell,j}(u), S_{r,j}(w) \right\} & \text{if } x = 0, \end{cases} \tag{4.2}$$

with

$$D_j(x,u) = H(x)D_{j,r}(u) + (1-H(x))D_{j,\ell}(u),$$
$$S_j(x,u) = H(x)S_{j,r}(u) + (1-H(x))S_{j,\ell}(u),$$

$D_{j,d}$ and $S_{j,d}$, $d = \ell, r$, defined as in (2.3).

The LWR model is numerically integrated through a Godunov type scheme, which provides the solution to the Cauchy problem (2.1) that maximises the flux through the junction:

- **1-to-1 junction (Section 4.2):**

$$\rho_k^{n+1} = \rho_k^n - \lambda \left[F(x_{k+1/2}, \rho_k^n, \rho_{k+1}^n) - F(x_{k-1/2}, \rho_{k-1}^n, \rho_k^n) \right], \tag{4.3}$$

  with F defined as in (4.2), omitting index j.
  In Section 4.2, we apply also a different strategy for the numerical integration of the LWR model: we make use of an upwind scheme, which provides the solution to the Cauchy problem (2.1) coming from the vanishing viscosity approach. The numerical scheme reads as in (4.3), where the numerical flux is now chosen as $F(x,u,w) = u\, v(x,w)$.

- **2-to-1 junction (Section 4.3):** we follow [12] so that, exploiting the notation introduced in (2.9), setting $\hat{\gamma}_i^n = \hat{\gamma}_i(\rho_{\ell_1,-1}^n, \rho_{\ell_2,-1}^n, \rho_{r,0}^n)$ for $i = \ell_1, \ell_2, r$, we have

$$\begin{aligned}
&\text{for } k < -1,\ \ell = \ell_1, \ell_2: && \rho_{\ell,k}^{n+1} = \rho_{\ell,k}^n - \lambda \left[F_\ell(\rho_{\ell,k}^n, \rho_{\ell,k+1}^n) - F_\ell(\rho_{\ell,k-1}^n, \rho_{\ell,k}^n) \right], \\
&\text{for } k > 1: && \rho_{r,k}^{n+1} = \rho_{r,k}^n - \lambda \left[F_r(\rho_{r,k}^n, \rho_{r,k+1}^n) - F_r(\rho_{r,k-1}^n, \rho_{r,k}^n) \right], \\
&\text{for } k = -1,\ \ell = \ell_1, \ell_2: && \rho_{\ell,-1}^{n+1} = \rho_{\ell,-1}^n - \lambda \left[\hat{\gamma}_\ell^n - F_\ell(\rho_{\ell,-2}^n, \rho_{\ell,-1}^n) \right], \\
&\text{for } k = 0: && \rho_{r,0}^{n+1} = \rho_{r,0}^n - \lambda \left[F_r(\rho_{r,0}^n, \rho_{r,1}^n) - \hat{\gamma}_r^n \right].
\end{aligned}$$

- **1-to-2 junction (Section 5):** as already recalled in Section 2.3, we use two different schemes, satisfying different rules at the junction.

  FIFO rule: we follow [10], and exploit the notation already introduced in (2.10), with $\gamma_i^n = \gamma_i(\rho_{\ell,-1}^n, \rho_{r_1,0}^n, \rho_{r_2,0}^n)$ for $i = \ell, r_1, r_2$.

  Non-FIFO rule: we follow [12] and exploit the notation already introduced in (2.11), with $\gamma_i^n = \gamma_i(\rho_{\ell,-1}^n, \rho_{r_1,0}^n, \rho_{r_2,0}^n)$ for $i = \ell, r_1, r_2$.

  For both rules, the scheme amounts to the following:

$$\begin{aligned}
&\text{for } k < -1: && \rho_{\ell,k}^{n+1} = \rho_{\ell,k}^n - \lambda \left[F_\ell(\rho_{\ell,k}^n, \rho_{\ell,k+1}^n) - F_\ell(\rho_{\ell,k-1}^n, \rho_{\ell,k}^n) \right], \\
&\text{for } k > 1,\ r = r_1, r_2: && \rho_{r,k}^{n+1} = \rho_{r,k}^n - \lambda \left[F_r(\rho_{r,k}^n, \rho_{r,k+1}^n) - F_r(\rho_{r,k-1}^n, \rho_{r,k}^n) \right], \\
&\text{for } k = -1: && \rho_{\ell,-1}^{n+1} = \rho_{\ell,-1}^n - \lambda \left[\gamma_\ell^n - F_\ell(\rho_{\ell,-2}^n, \rho_{\ell,-1}^n) \right], \\
&\text{for } k = 0,\ r = r_1, r_2: && \rho_{r,0}^{n+1} = \rho_{r,0}^n - \lambda \left[F_r(\rho_{r,0}^n, \rho_{r,1}^n) - \gamma_r^n \right],
\end{aligned}$$

  with the above choices of γ_i^n, $i = \ell, r_1, r_2$.

4.2 1-to-1 junction: from 2 to 3 lanes

We consider the case of a junction with one incoming road with 2 lanes and one outgoing road with 3 lanes. For the multilane model, this corresponds to problem (3.1)–(3.5)–(3.8) with $\mathcal{M}_\ell = \{1, 2\}$, $\mathcal{M}_r = \{1, 2, 3\}$ and $S_{\ell,2}(u, w) = 0$. For the LWR model, this is a 1-to-1 junction with maximal density on $]-\infty, 0[$ equal to $M_\ell = 2$, while on $]0, +\infty[$ it is $M_r = 3$.

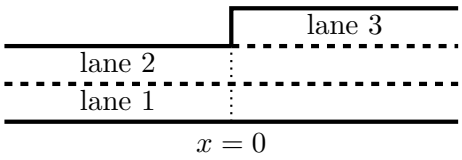

Case 1. We choose $V_\ell = 1.5$, $V_r = 1$. The initial datum for the multilane model is

$$\rho_{o,1}(x) = 0.6, \qquad \rho_{o,2}(x) = 0.4, \qquad \rho_{o,3}(x) = 0.5 * \chi_{[0,+\infty[}(x), \tag{4.4}$$

while the initial datum for the LWR model is given by the sum of the above functions, thus

$$\rho_o(x) = 1 * \chi_{]-\infty,0[}(x) + 1.5 * \chi_{[0,+\infty[}(x),$$

corresponding to the critical densities of the flux functions f_ℓ and f_r respectively, see Figure 3, i.e. the points where the flux functions attain their unique global maximum.

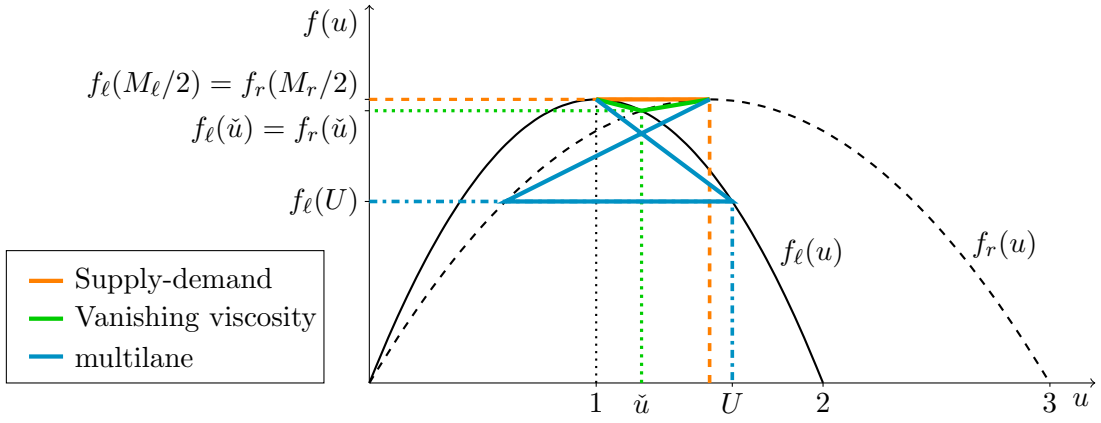

Figure 3: Flux functions f_ℓ and f_r related to the LWR model, for $M_\ell = 2$, $M_r = 3$, $V_\ell = 1.5$ and $V_r = 1$. The point $\check{u}$ is such that $f_\ell(\check{u}) = f_r(\check{u})$. The value U corresponds to the left trace at $x = 0$ of the sum of the solutions of the multilane model on the two incoming lanes, and $f_\ell(U)$ is the corresponding value of the flux.

Figure 4, left, displays the solutions of the considered models at time $t = 1$: in particular, it allows to compare the multilane model, namely the sum of the densities on the various lanes, to the LWR model. For the latter, there are many admissible solutions: indeed, depending on the physics of the problem, the solution may be different, see [3] and references therein for a thorough discussion on the choice of the "right" solution and on the physical models behind. In particular, the solutions obtained through the Godunov type scheme and through

the upwind scheme are different. The former, obtained via the Godunov type scheme and thus through an *ad hoc* minimisation between the demand and supply function, is the solution that maximises the flux at $x = 0$, i.e. at the point of discontinuity of the flux: the solution connects $f_\ell(M_l/2)$ and $f_r(M_r/2)$, see also Figure 3. On the other hand, the intermediate value attained around $x = 0$ by the solution coming from the upwind scheme corresponds to the point $\check{u}$ in Figure 3: this point is such that $f_\ell(\check{u}) = f_r(\check{u})$. When higher order effects are taken into account for choosing the "right" solution, the choice of the vanishing viscosity approximation leads to this particular solution.

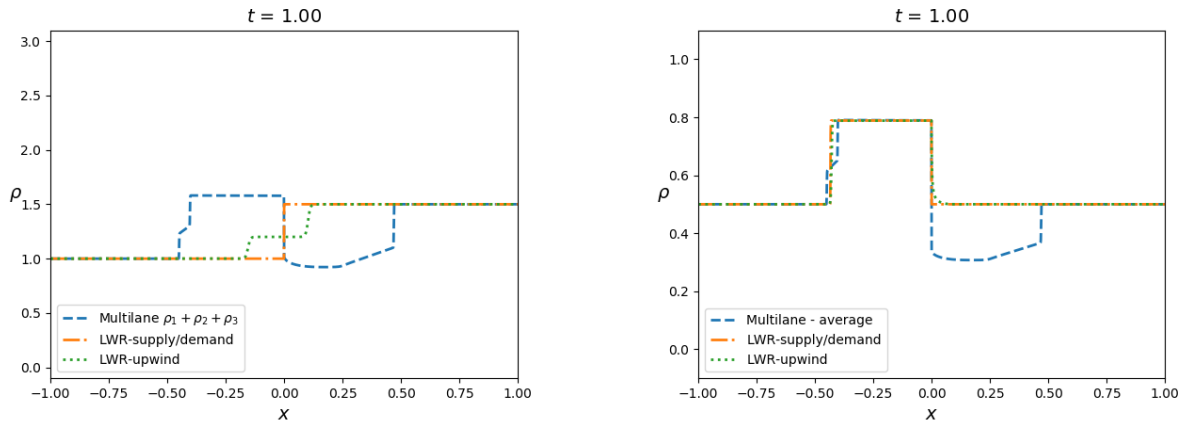

Figure 4: The dashed blue line corresponds to the multilane model (3.1)–(3.5)–(3.8): on the left, it is the sum of its solutions, on the right it is the average. The dash-dotted orange line corresponds to the solution to the LWR model (2.1) obtained via the Godunov type scheme; the dotted green line is the solution to the LWR model (2.1) obtained through the upwind scheme. Here: $V_\ell = 1.5$, $V_r = 1$, initial datum (4.4).

Concerning the solution of the multilane model, the low value of the sum of the densities right downstream $x = 0$ is due to the fact that, before $x = 0$, the third lane does not exist. Thus, even though vehicles pass from the second to the third lane, the solution in the third lane is given by a shock with positive speed. On the other hand, the *queue* right upstream $x = 0$ is caused by the congestion of lanes 1 and 2, since after $x = 0$ the maximal speed decreases. Moreover, notice that the solution of the multilane model maximises the flux on each lane at the junction, see also Figure 5, right.

We make a second comparison between the LWR and the multilane model, namely we take the latter in the form of the average of the densities on the various lanes. In this way, the maximal density for the LWR model equals 1 everywhere. The initial datum is therefore given by the average of (4.4):

$$\rho_o(x) = 0.5,$$

which corresponds to the critical density of the flux function on both incoming and outgoing lanes. Figure 4, right, displays the solutions at time $t = 1$. We notice how the solutions resemble each other on the incoming lane: the queue upstream $x = 0$ is well captured by all models. On the other hand, also in this case the behaviour of the multilane model on the outgoing lane strongly differs from the LWR model, for which in this case the supply-demand and the vanishing viscosity solutions coincide.

Recall that, by [13, Lemma 2.3], the multilane model (3.1)–(3.5)–(3.8) preserves the total number of vehicles over time. This property is clearly valid when considering the multilane model in the form of the sum of densities on the various lanes. However, this second type of comparison considering the average of the densities on the various lanes implies that the total number of vehicles is not conserved anymore through the junction: indeed, the total mass is divided by the number of lanes, which is equal to 2 upstream $x = 0$ and 3 downstream.

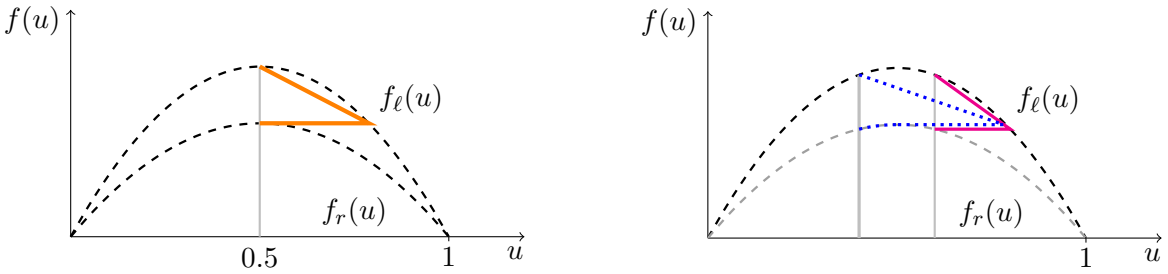

Figure 5: Left: Flux functions f_ℓ and f_r related to the LWR model when comparing it to the multilane model in the form of the average of the densities on the various lanes: $V_\ell = 1.5$ and $V_r = 1$, in both cases the maximal density is 1. The orange line represents the solution to the Riemann problem with initial datum $\rho_o(x) = 0.5$. Right: flux functions related to the multilane model for the incoming (f_ℓ) and the outgoing (f_r) lanes. The magenta line represents the solution on lane 1, with initial datum $\rho_{o,1} = 0.6$; the dotted blue line corresponds to the solution on lane 2, with initial datum $\rho_{o,2} = 0.4$.

Case 2. We choose now $V_\ell = 1$ and $V_r = 1.5$ and the same initial data of Case 1. The flux functions for the LWR model are displayed in Figure 6. In this case, the solution obtained with the Godunov type scheme is identical to that obtained through the upwind method, see Figure 7. Notice that the stationary shock at $x = 0$ is slightly smoothed out when using the upwind scheme, due to numerical viscosity. The small slope right before $x = 0$ in the sum of the solutions to the multilane model is caused by the higher flux of vehicles in lane 2 through $x = 0$, since right after $x = 0$ the speed is higher and vehicles can pass also in lane 3.

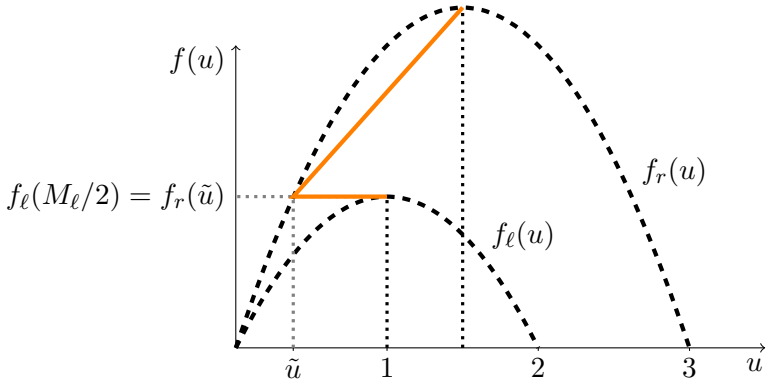

Figure 6: Flux functions f_ℓ and f_r related to the LWR model, for $M_\ell = 2$, $M_r = 3$, $V_\ell = 1$ and $V_r = 1.5$. The point $\tilde{u}$ is such that $f_r(\tilde{u}) = f_\ell(1)$.

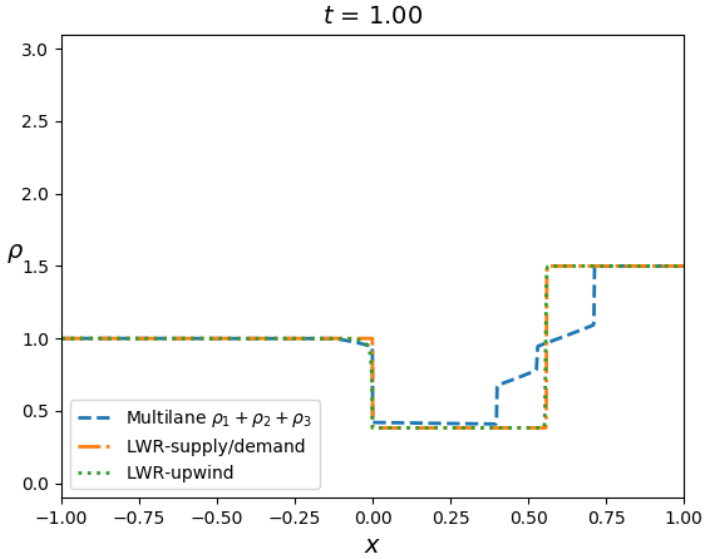

Figure 7: The dashed blue line is the sum of the solutions to the multilane model (3.1)–(3.5)–(3.8); the dash-dotted orange line corresponds to the solution to the LWR model (2.1) obtained via the Godunov type scheme; the dotted green line is the solution to the LWR model (2.1) obtained through the upwind scheme. Here: $V_\ell = 1$, $V_r = 1.5$, initial datum (4.4).

4.3 2-to-1 junction: from 2+2 to 2 lanes

We consider the case of a junction consisting of two incoming roads with 2 lanes each and one outgoing road with 2 lanes, that is problem (3.1)–(3.6)–(3.8), with $\mathcal{M}_\ell = \{1, 2, 3, 4\}$, $\mathcal{M}_r = \{2, 3\}$ and initial data

$$\begin{aligned} &\rho_{o,1}(x) = 0.6\,\chi_{]-\infty,0]}(x) + 1\,\chi_{]0,+\infty[}(x), \quad \rho_{o,2}(x) = 0.4, \\ &\rho_{o,3}(x) = 0.6\chi_{]-\infty,0]}(x) + 0.8\,\chi_{]0,+\infty[}(x), \quad \rho_{o,4}(x) = 0.4\,\chi_{]-\infty,0]}(x) + 1\,\chi_{]0,+\infty[}(x), \end{aligned} \tag{4.5}$$

with the additional assumption that there is no flow of vehicles between the second and the third lane on $]-\infty, 0[$, i.e. $S_{\ell,2}(u, w) = 0$ (we also impose $S_{r,1}(u, w) = S_{r,3}(u, w) = 0$). The situation under consideration looks as follows:

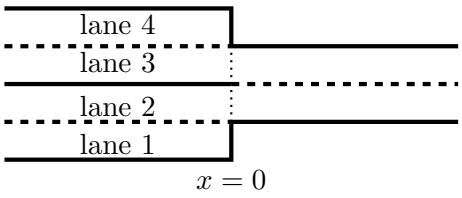

Concerning the LWR model, we denote by ℓ_1 and ℓ_2 the two incoming roads, and by r the outgoing one. Then, the initial data for problem (2.1) corresponding to (4.5) read as follows:

$$\rho_{o,\ell_1}(x) = 1, \qquad \rho_{o,\ell_2}(x) = 1, \qquad \rho_{o,r}(x) = 1.2, \tag{4.6}$$

since road ℓ_1 is given by lanes 1 and 2 for $x \in]-\infty, 0[$, road ℓ_2 is given by lanes 3 and 4 for $x \in]-\infty, 0[$ and road r is given by lanes 2 and 3 for $x \in]0, +\infty[$. Moreover, we prescribe the priority $P = 1 - P = 1/2$ on each incoming road. Observe that the maximal density on each road is equal to 2.

Figure 8 displays the solution on each road at time $t = 1$: in each picture we can see both the LWR model and the multilane model, in the form of the sum of the densities on the involved lanes. Notice the asymmetric behaviour of the multilane model: this is due to the asymmetry of the initial data (4.5) with respect to the lanes that are left after the junction. Indeed, the initial datum in lane 2 has a lower value than in lane 1, while the opposite is true for lane 3 with respect to lane 4. In the former case, this implies that more vehicles have to pass form lane 1 to lane 2 in order to go through the junction, causing the formation of a longer queue, which become visible when summing the two densities, see Figure 8. Figure 9 provides a detail of the multilane model at the same time $t = 1$, allowing a better insight on the queue formation.

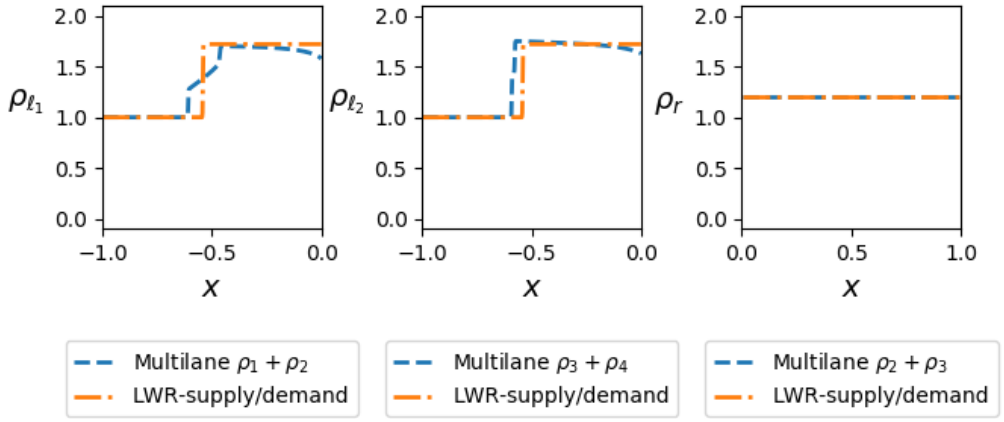

Figure 8: In each picture, the dashed blue line is the sum of the solutions to the multilane model (3.1)–(3.5)–(3.8): from left to right, lanes 1 and 2; lanes 3 and 4; lanes 2 and 3. The dash-dotted orange line corresponds to the solution to the LWR model (2.1), obtained through a Godunov type scheme, with priorities $(1/2, 1/2)$: from left to right, incoming roads a, b, outgoing road c. The initial data are given in (4.5) and (4.6) respectively. In each lane we set $V = 1.5$.

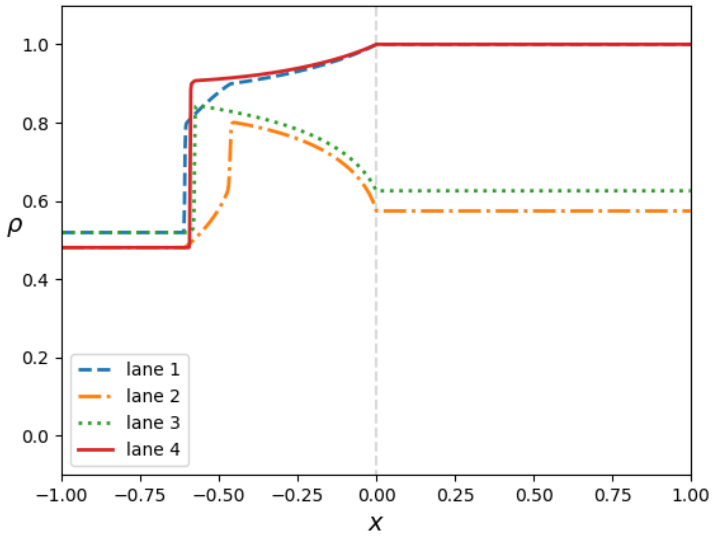

Figure 9: Solution to the multilane model (3.1)–(3.5)–(3.8) at time $t = 1$, with initial data (4.5) and $V = 1.5$ on each lane.

5 A multilane model for a diverge

In this section, we aim to compare the LWR model on a one-to-two (diverging) junction with a multilane model different from the one considered in Section 3. Indeed, we need to account for the drivers' routing preferences upstream, a feature that is not included in the multilane model (3.1)–(3.7).

The specific multilane junction looks as follows: there are one incoming road with two lanes and two outgoing roads, with one lane each.

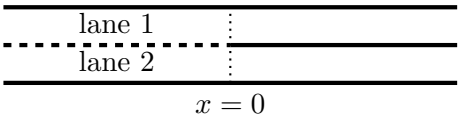

The core idea is to consider a multi-population model [4, 9], where each population is identified by its desired final destination. In the particular case under consideration, we have two populations, which coexist upstream $x = 0$. We assume that, in each lane of the incoming road, a fraction α of the drivers belong to the first population, i.e. wants to go in lane 1 downstream $x = 0$, while the rest is directed towards lane 2. Overtaking is possible only upstream $x = 0$, and, differently from the multilane model considered in Section 3, only vehicles in lane 1 (respectively lane 2) targeting lane 2 (respectively lane 1) change lane. The rate of vehicles changing lane depends on the total density in the target lane: the more the target lane is crowded, the less vehicles are allowed to move into that lane. Moreover, the *desire* to go in the target lane increases as drivers approach the junction ($x = 0$). Since we focus on the dynamics at the junction, we do not consider the classical overtaking dynamics, which can occur before $x = 0$. This could be added in the source term with minor changes in the overall approach.

Our multilane multi-population model is the following: given the initial data $\rho_{o,1}$ and $\rho_{o,2}$ on $\mathbb{R}$, the initial data on $x < 0$ read

$$\begin{aligned} &\rho^1_{o,1}(x) = \alpha\,\rho_{o,1}(x)\,\chi_{]-\infty,0]}(x), \quad \rho^2_{o,1}(x) = (1-\alpha)\,\rho_{o,1}(x)\,\chi_{]-\infty,0]}(x), \\ &\rho^1_{o,2}(x) = \alpha\,\rho_{o,2}(x)\,\chi_{]-\infty,0]}(x), \quad \rho^2_{o,2}(x) = (1-\alpha)\,\rho_{o,2}(x)\,\chi_{]-\infty,0]}(x), \end{aligned} \tag{5.1}$$

where $\rho^i_{o,j}$, for $i, j \in \{1, 2\}$, denotes the amount of drivers in lane j targeting lane i. Setting $\rho_1 = \rho^1_1 + \rho^2_1$ and $\rho_2 = \rho^1_2 + \rho^2_2$, the densities ρ^i_j, $i, j = 1, 2$, satisfy the following system:

$$\begin{cases} \partial_t \rho^1_1 + \partial_x \left(\rho^1_1\, v_1(\rho_1)\right) = K\,\rho^1_2\,\dfrac{\max\{1-\rho_1, 0\}}{|x|}\,\chi_{]-\infty,0[}(x) \\ \partial_t \rho^2_1 + \partial_x \left(\rho^2_1\, v_1(\rho_1)\right) = -K\,\rho^2_1\,\dfrac{\max\{1-\rho_2, 0\}}{|x|}\,\chi_{]-\infty,0[}(x) \\ \partial_t \rho^1_2 + \partial_x \left(\rho^1_2\, v_2(\rho_2)\right) = -K\,\rho^1_2\,\dfrac{\max\{1-\rho_1, 0\}}{|x|}\,\chi_{]-\infty,0[}(x) \\ \partial_t \rho^2_2 + \partial_x \left(\rho^2_2\, v_2(\rho_2)\right) = K\,\rho^2_1\,\dfrac{\max\{1-\rho_2, 0\}}{|x|}\,\chi_{]-\infty,0[}(x), \end{cases} \tag{5.2}$$

where K is a dimensional constant (m/s), which can be assumed equal to 1 after rescaling space and time. In the source terms, the factor $|x|^{-1}$ represents the increase of the urgency to change lane as the junction approaches.

We observe that a close model which describes traffic on a multilane highway under the hypotheses that traffic is neither perfectly FIFO nor perfectly non-FIFO has been introduced in [20]. Here, we compare the multilane multi-population model (5.2) to the LWR model for a diverging junction, both in the case of a FIFO rule and of a non-FIFO rule at the junction, see Section 2.3. The incoming roads are paired together, and denoted by the subscript ℓ, while

the two distinct outgoing roads are denoted by subscripts r_1 and r_2 respectively. The initial data for problem (2.1) is related to the initial data $\rho_{o,1}, \rho_{o,2}$ for the multilane multi-population model as follows:

$$\begin{aligned}
\rho_{o,\ell}(x) &= \big(\rho_{o,1}(x) + \rho_{o,2}(x)\big)\, \chi_{]-\infty,0]}(x), \\
\rho_{o,r_1}(x) &= \rho_{o,1}(x)\, \chi_{]0,+\infty[}(x), \\
\rho_{o,r_2}(x) &= \rho_{o,2}(x)\, \chi_{]0,+\infty[}(x).
\end{aligned} \tag{5.3}$$

5.1 Numerical scheme

We detail here the numerical scheme exploited for the integration of the multilane multi-population model (5.2). The scheme is inspired by that presented in [7, 19], and the source terms are treated through fractional step.

The space and time mesh are defined as in Section 4.1. The initial data on each lane, $\rho_{o,1}$ and $\rho_{o,2}$, are approximated by $\rho^0_{1,k}$ and $\rho^0_{2,k}$, for $k \in \mathbb{Z}$, as in (4.1), then distinguished on the negative part of the x-axis according to their target lane: for $k \le -1$

$$\begin{aligned}
\rho^{1,0}_{1,k} &= \alpha\, \rho^0_{1,k}, & \rho^{2,0}_{1,k} &= (1-\alpha)\rho^0_{1,k}, \\
\rho^{1,0}_{2,k} &= \alpha\, \rho^0_{2,k}, & \rho^{2,0}_{2,k} &= (1-\alpha)\rho^0_{2,k}.
\end{aligned}$$

The solution to the multilane multi-population model (5.2) is obtained through a Godunov type scheme, with fractional step to account for the source terms. In particular, set $\rho^n_{j,k} = \rho^{1,n}_{j,k} + \rho^{2,n}_{j,k}$ and introduce the quantity $\gamma^n_j = \min\Big\{\hat D_j(\rho^{j,n}_{j,-1}, \rho^{i,n}_{j,-1}), S_j(\rho^n_{j,0})\Big\}$, for $j = 1, 2$, $i = 3 - j$, with S_j as in (2.3) and $\hat D_j$ defined as let $\vartheta_j(w)$ the point of maximum of the function $u \mapsto u v_j(u + w)$, then

$$\hat D_j(u, w) = \begin{cases} u\, v_j(u + w) & \text{if } u < \vartheta_j(w), \\ \vartheta_j(w)\, v_j\big(\vartheta_j(w) + w\big) & \text{if } u \ge \vartheta_j(w). \end{cases}$$

Then, for i, $j = 1, 2$, we set

$$\begin{aligned}
&\text{if } k < -1: && \rho^{i,n+1/2}_{j,k} = \rho^{i,n}_{j,k} - \lambda \left[\frac{\rho^{i,n}_{j,k}}{\rho^n_{j,k}} F(\rho^n_{j,k}, \rho^n_{j,k+1}) - \frac{\rho^{i,n}_{j,k-1}}{\rho^n_{j,k-1}} F(\rho^n_{j,k-1}, \rho^n_{j,k}) \right], \\
&\text{if } k = -1: && \rho^{i,n+1/2}_{j,-1} = \rho^{i,n}_{j,-1} - \lambda \left[\gamma^n_j - \frac{\rho^{i,n}_{j,-2}}{\rho^n_{j,-2}} F(\rho^n_{j,-2}, \rho^n_{j,-1}) \right], \\
&\text{if } k = 0: && \rho^{n+1}_{j,0} = \rho^n_{j,0} - \lambda \Big[F(\rho^n_{j,0}, \rho^n_{j,1}) - \gamma^n_j \Big], \\
&\text{if } k > 0: && \rho^{n+1}_{j,k} = \rho^n_{j,k} - \lambda \Big[F(\rho^n_{j,k}, \rho^n_{j,k+1}) - F(\rho^n_{j,k-1}, \rho^n_{j,k}) \Big],
\end{aligned}$$

with $F(u, w) = \min\Big\{\hat D_j(u), S_j(w)\Big\}$. Concerning the contribution of the source terms, define

$$G(x, u, w) = w\, \frac{\max\{1 - u, 0\}}{|x|}\, \chi_{]-\infty,0[}(x)$$

so that

$$\begin{aligned}
\rho_{1,k}^{1,n+1} &= \rho_{1,k}^{1,n+1/2} + \Delta t\, G(x_k, \rho_{1,k}^{n+1/2}, \rho_{2,k}^{1,n+1/2}),\\
\rho_{1,k}^{2,n+1} &= \rho_{1,k}^{2,n+1/2} - \Delta t\, G(x_k, \rho_{2,k}^{n+1/2}, \rho_{1,k}^{2,n+1/2}),\\
\rho_{2,k}^{1,n+1} &= \rho_{2,k}^{1,n+1/2} - \Delta t\, G(x_k, \rho_{1,k}^{n+1/2}, \rho_{2,k}^{1,n+1/2}),\\
\rho_{2,k}^{2,n+1} &= \rho_{2,k}^{2,n+1/2} + \Delta t\, G(x_k, \rho_{2,k}^{n+1/2}, \rho_{1,k}^{2,n+1/2}).
\end{aligned}$$

5.2 Example 1: fully congested outgoing road

The first example we take into account considers a fully congested outgoing road. We choose $\alpha = 0.4$, the maximal speed on the incoming road is $V_\ell = 1.5$ and on both outgoing roads it is $V_r = 2$. The initial data for the multilane multi-population model (5.2) are

$$\begin{aligned}
\rho_{o,1}(x) &= 0.6\, \chi_{]-\infty,0]}(x) + 0.4\, \chi_{]0,+\infty[}(x),\\
\rho_{o,2}(x) &= 0.7\, \chi_{]-\infty,0]}(x) + 1\, \chi_{]0,+\infty[}(x),
\end{aligned} \tag{5.4}$$

and through (5.3) we recover the initial data for the corresponding LWR model (2.1).

Figure 10 displays the solution on each road at time $t = 0.5$: in each picture we see the LWR model with both FIFO and non-FIFO rule and the multilane multi-population model, in the form of the sum of the densities for $x < 0$. Lane 2 is initially fully congested: no vehicles can enter, and the solution on that lane is clearly the same with all the three models. In this situation, the solution of the multilane multi-population model looks very close to that of the LWR model with FIFO rule. Indeed, non-FIFO rule allows vehicles targeting lane 1 to overcome the junction: they are not queuing waiting for their turn to pass the junction.

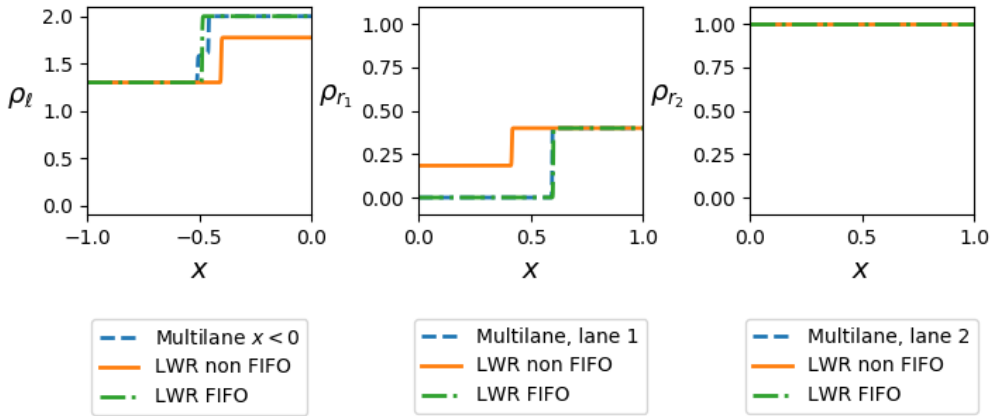

Figure 10: In each picture, the dashed blue line corresponds to the solutions to the multilane multi-population model (5.2), and in particular to their sum on $x < 0$. The dotted orange line corresponds to the solution of the LWR model (2.1) with non-FIFO rule, while the dash-dotted green line is the solution to the LWR model (2.1) with FIFO rule. The initial data is (5.4), while $V_\ell = 1.5$, $V_r = 2$ and $\alpha = 0.4$.

5.3 Example 2

In this second example, none of the outgoing lane is fully congested. We keep the same parameters as before, thus $\alpha = 0.4$, $V_\ell = 1.5$, $V_r = 2$. The initial data for the multilane multi-population model (5.2) are

$$\begin{aligned} \rho_{o,1}(x) &= 0.6\,\chi_{]-\infty,0]}(x) + 0.4\,\chi_{]0,+\infty[}(x), \\ \rho_{o,2}(x) &= 0.7\,\chi_{]-\infty,0]}(x) + 0.8\,\chi_{]0,+\infty[}(x), \end{aligned} \tag{5.5}$$

which differ from (5.4) only in the density on the second road downstream $x = 0$. Through (5.3) we recover the initial data for the LWR model (2.1).

Figure 11 displays the solution on each road at time $t = 0.5$: in each picture we see the LWR model with both FIFO and non-FIFO rule and the multilane multi-population model, in the form of the sum of the densities for $x < 0$. Even though lane 2 is not fully congested downstream $x = 0$, all the three models produce the same solution there. However, on the outgoing road corresponding to lane 1 the solution to the multilane multi-population model (5.2) is very close to the solution to the LWR model (2.1) with non-FIFO rule. In the incoming roads, the similarity is reduced, but nevertheless the solution to the LWR model with FIFO rule looks much different than the others, since it reaches a greater value upstream $x = 0$.

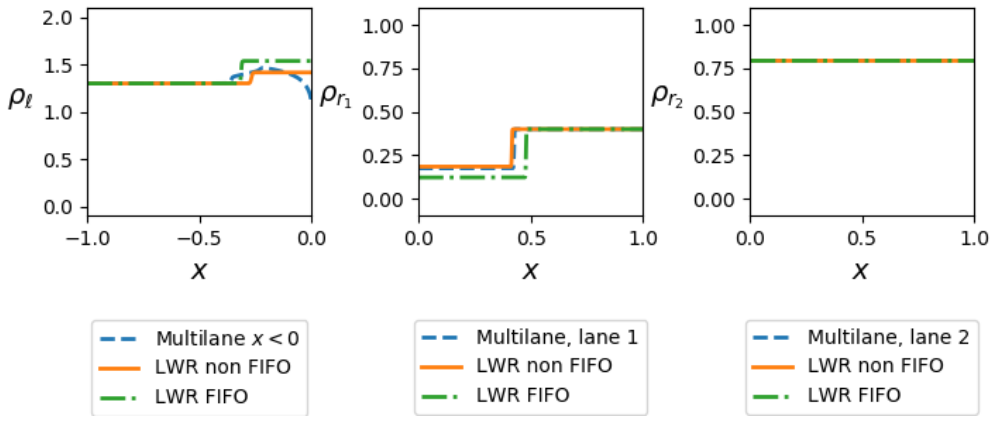

Figure 11: In each picture, the dashed blue line corresponds to the solutions to the multilane multi-population model (5.2), and in particular to their sum on $x < 0$. The dotted orange line corresponds to the solution of the LWR model (2.1) with non-FIFO rule, while the dash-dotted green line is the solution to the LWR model (2.1) with FIFO rule. The initial data is (5.5), while $V_\ell = 1.5$, $V_r = 2$ and $\alpha = 0.4$.

References

[1] Adimurthi and G. D. V. Gowda. Conservation law with discontinuous flux. *J. Math. Kyoto Univ.*, 43(1):27–70, 2003.

[2] Adimurthi, J. Jaffré, and G. D. Veerappa Gowda. Godunov-type methods for conservation laws with a flux function discontinuous in space. *SIAM J. Numer. Anal.*, 42(1):179–208, 2004.

[3] Adimurthi, S. Mishra, and G. D. V. Gowda. Optimal entropy solutions for conservation laws with discontinuous flux-functions. *J. Hyperbolic Differ. Equ.*, 2(4):783–837, 2005.

[4] E. Cristiani and F. S. Priuli. A destination-preserving model for simulating Wardrop equilibria in traffic flow on networks. *Netw. Heterog. Media*, 10(4):857–876, 2015.

[5] S. Diehl. On scalar conservation laws with point source and discontinuous flux function. *SIAM J. Math. Anal.*, 26(6):1425–1451, 1995.

[6] S. Diehl. Scalar conservation laws with discontinuous flux function. I. The viscous profile condition. *Comm. Math. Phys.*, 176(1):23–44, 1996.

[7] A. Festa and P. Goatin. Modeling the impact of on-line navigation devices in traffic flows. In *58th IEEE Conference on Decision and Control*, Nice, France, Dec. 2019.

[8] M. Garavello, K. Han, and B. Piccoli. *Models for vehicular traffic on networks*, volume 9 of *AIMS Series on Applied Mathematics*. American Institute of Mathematical Sciences (AIMS), Springfield, MO, 2016.

[9] M. Garavello and B. Piccoli. Source-destination flow on a road network. *Commun. Math. Sci.*, 3(3):261–283, 2005.

[10] M. Garavello and B. Piccoli. *Traffic flow on networks*, volume 1 of *AIMS Series on Applied Mathematics*. American Institute of Mathematical Sciences (AIMS), Springfield, MO, 2006. Conservation laws models.

[11] T. Gimse and N. H. Risebro. Solution of the Cauchy problem for a conservation law with a discontinuous flux function. *SIAM J. Math. Anal.*, 23(3):635–648, 1992.

[12] P. Goatin, S. Göttlich, and O. Kolb. Speed limit and ramp meter control for traffic flow networks. *Eng. Optim.*, 48(7):1121–1144, 2016.

[13] P. Goatin and E. Rossi. A multilane macroscopic traffic flow model for simple networks. *SIAM J. Appl. Math.*, 79(5):1967–1989, 2019.

[14] H. Holden and N. H. Risebro. *Front tracking for hyperbolic conservation laws*, volume 152 of *Applied Mathematical Sciences*. Springer, Heidelberg, second edition, 2015.

[15] H. Holden and N. H. Risebro. Models for dense multilane vehicular traffic. *SIAM J. Math. Anal.*, 51(5):3694–3713, 2019.

[16] K. H. Karlsen, N. H. Risebro, and J. D. Towers. L^1 stability for entropy solutions of nonlinear degenerate parabolic convection-diffusion equations with discontinuous coefficients. *Skr. K. Nor. Vidensk. Selsk.*, 3:1–49, 2003.

[17] M. J. Lighthill and G. B. Whitham. On kinematic waves. II. A theory of traffic flow on long crowded roads. *Proc. Roy. Soc. London. Ser. A.*, 229:317–345, 1955.

[18] P. I. Richards. Shock waves on the highway. *Operations Res.*, 4:42–51, 1956.

[19] S. Samaranayake, W. Krichene, J. Reilly, M. L. D. Monache, P. Goatin, and A. Bayen. Discrete-time system optimal dynamic traffic assignment (SO-DTA) with partial control for physical queuing networks. *Transportation Science*, 52(4):982–1001, 2018.

[20] B. Schnetzler, X. Louis, and J.-P. Lebacque. A multilane junction model. *TRANSPORTMETRICA*, 8(4):243–260, 2012.

[21] J. D. Towers. Convergence of a difference scheme for conservation laws with a discontinuous flux. *SIAM J. Numer. Anal.*, 38(2):681–698, 2000.